The Canadian Mineralogist
Vol. 41, pp. 1413-1422 (2003)

THE STRUCTURE OF DANALITE AT HIGH TEMPERATURE OBTAINED FROM SYNCHROTRON RADIATION AND RIETVELD REFINEMENTS

SYTLE M. ANTAO[§]

Mineral Physics Institute and Department of Geosciences, State University of New York, Stony Brook, New York, N.Y. 11794-2100, U.S.A.

ISHMAEL HASSAN

Department of Chemistry, University of the West Indies, Mona, Kingston 7, Jamaica

JOHN B. PARISE

Mineral Physics Institute and Department of Geosciences, State University of New York, Stony Brook, New York, N.Y. 11794-2100, U.S.A.

ABSTRACT

The structural behavior of danalite, ideally $Fe_8[Be_6Si_6O_{24}]S_2$, at atmospheric pressure and from 33 to 1035°C on heating, was determined by using *in situ* synchrotron X-ray powder-diffraction data ($\lambda = 0.92249$ Å) and Rietveld refinement. The sample was heated at a rate of about 9.5°C/min., and X-ray traces were collected at about 18°C intervals. The unit-cell parameter for danalite increases linearly to 1035°C. The percent change in volume between 33 and 1035°C is 1.6(1)%. Other structural parameters show an abrupt change at about 926°C. Between 33 and 926°C, the Be–O and Si–O distances are nearly constant. Between 926 and 1035°C, the Be–O bond length decreases, whereas the Si–O bond distance increases, but the changes are small. From 33 to 926°C, the Be–O–Si angle increases by 1.12(3)°, and the total increase up to 1035°C is 1.21(3)°. Simultaneously, between 33 and 926°C, both the angles of rotation of the BeO_4 (φ_{Be}) and SiO_4 (φ_{Si}) tetrahedra decrease by about 0.71°, respectively. From 926 to 1035°C, both φ_{Be} and φ_{Si} increase by about 0.23°. The Fe–S bond length increases by 0.023(1) Å from 33 to 926°C, and by 0.007(1) Å from 926 to 1035°C. The Fe–O bond distance increases by 0.024(1) Å from 33 to 926°C, and decreases by 0.001(1) Å from 926 to 1035°C. Large displacement-parameters occur for the Fe and S atoms, and as the Fe–S bond expands with temperature, the Fe atoms move toward the plane of the six-membered rings in the framework, which causes the tetrahedra to rotate slightly and results in the expansion of the structure. The abrupt change in structural parameters probably occurs because of the oxidation of Fe^{2+} (and minor Mn^{2+}) cations beyond 771°C, and the loss of S_2(g) beyond 1029°C.

Keywords: danalite, high-temperature structure, synchrotron radiation, Rietveld refinements.

SOMMAIRE

Nous avons étudié le comportement structural de la danalite, de composition idéale $Fe_8[Be_6Si_6O_{24}]S_2$, à pression atmosphérique lors d'un chauffage de 33 à 1035°C, en utilisant des données de diffraction X sur poudres générées *in situ* avec rayonnement synchrotron ($\lambda = 0.92249$ Å) et traitées par affinement de Rietveld. L'échantillon a été chauffé à un taux d'environ 9.5°C/min., et les tracés des spectres ont été prélevés à des intervalles de 18°C environ. Le paramètre réticulaire de la danalite augmente de façon linéaire jusqu'à 1035°C. Le taux de changement de son volume entre 33 et 1035°C est 1.6(1)%. Les autres paramètres structuraux font preuve d'un changement abrupt à environ 926°C. Entre 33 et 926°C, les distances Be–O et Si–O demeurent presque constantes. Entre 926 et 1035°C, la longueur de la liaison Be–O diminue, tandis que celle de la liaison Si–O augmente, mais les changements sont faibles. Entre 33 et 926°C, l'angle Be–O–Si augmente de 1.12(3)°, et l'augmentation totale jusqu'à 1035°C est 1.21(3)°. En même temps, entre 33 et 926°C, les angles de rotation des tétraèdres BeO_4 (φ_{Be}) et SiO_4 (φ_{Si}) diminuent d'environ 0.71°, respectivement. Entre 926 et 1035°C, φ_{Be} et φ_{Si} augmentent d'environ 0.23°. La liaison Fe–S augmente en longueur de 0.023(1) Å entre 33 et 926°C, et de 0.007(1) Å entre 926 et 1035°C. La liaison Fe–O augmente en longueur de 0.024(1) Å entre 33 et 926°C, et diminue de 0.001(1) Å entre 926 et 1035°C. Les coefficients de déplacement des atomes Fe et S sont importants, et la liaison Fe–S s'allonge avec la température, les atomes de Fe se rapprochant progressivement du plan des anneaux à six membres dans la trame, ce qui cause une légère rotation des tétraèdres, et mène à une expansion de la structure. Le

§ *E-mail address*: sytle.antao@stonybrook.edu

changement abrupt des paramètres structuraux a probablement lieu à cause de l'oxydation des cations Fe^{2+} (et, en quantité moindre, Mn^{2+}) au delà de 771°C, et la perte de S_2(g) au delà de 1029°C.

(Traduit par la Rédaction)

Mots-clés: danalite, structure à température élevée, rayonnement synchrotron, affinement de Rietveld.

Introduction

Danalite belongs to the helvite group of minerals, $(Mn,Fe,Zn)_8[Be_6Si_6O_{24}]S_2$, and is the Fe-rich member. Barth (1926) and Gottfried (1927) determined the space group of helvite, and Pauling (1930) determined its structure. The structure of helvite was subsequently refined by Holloway *et al.* (1972). Dunn (1976) chemically analyzed helvite-group minerals, including danalite, from numerous localities. Danalite was the only end-member of the helvite group that could not be synthesized by Mel'nikov *et al.* (1968). The room-temperature structure of danalite (space group $P\bar{4}3n$), ideally $Fe_8[Be_6Si_6O_{24}]S_2$, was refined by Hassan & Grundy (1985).

The structure of danalite has not been previously studied at high temperature. The present study was carried out to determine the structural behavior of danalite to 1035°C using *in situ* synchrotron X-ray powder-diffraction data and Rietveld refinement of the structure. The thermal expansion of danalite is also discussed in terms of the observed structural changes and the geometrical model of Hassan & Grundy (1984). The results for danalite are compared to those for sodalite (Hassan *et al.* 2004).

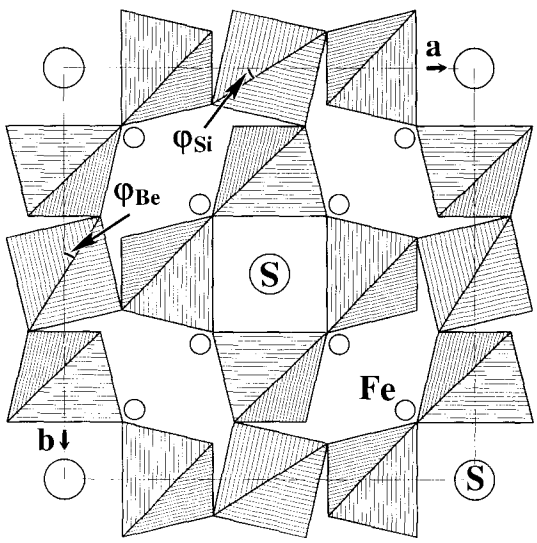

FIG. 1. Projection of the structure of danalite down [001] showing the lower half of the unit cell. The Be and Si tetrahedra alternate in the rings, and the angles of rotation of these tetrahedra are indicated by φ_{Be} and φ_{Si}, which also serve to identify the TO_4 tetrahedra. The S atom is shown as large circles, and the Fe^{2+} cations as smaller circles.

Background Information

The helvite-group minerals are isotypic with sodalite, $Na_8[Al_6Si_6O_{24}]Cl_2$. The framework structure is characterized by four-membered rings in the faces of the unit cell, and these rings are linked to form six-membered rings about the corners of the unit cell (Fig. 1). The Si and Be atoms alternate in these rings, as they are ordered. The sodalite or β-cage (using zeolite nomenclature) in danalite encloses $[Fe_4{\bullet}S]^{6+}$ clusters. The S atoms are at the corners and center of the unit cell, and the Fe atoms are on the threefold axes adjacent to the six-membered rings. The S atom is tetrahedrally coordinated by four Fe atoms, whereas the Fe atom is in fourfold coordination, surrounded by one S atom and three framework O atoms. The $[Fe_4{\bullet}S]^{6+}$ clusters in danalite are highly charged (*i.e.*, 6+ valence units), so they have smaller sizes compared to the $[Na_4{\bullet}Cl]^{3+}$ clusters in sodalite and tugtupite (Hassan & Grundy 1985, 1991). In addition, danalite contains Be^{2+} instead of the larger Al^{3+} cations in sodalite ($^{[4]}$Be: r = 0.27 Å; $^{[4]}$Al: r = 0.39 Å; Shannon 1976), so the danalite framework is in a highly collapsed state compared to that of sodalite.

Experimental Methods

The sample of danalite used in this study is from the Mt. Francisco granitic pegmatite, Ribawa area, Western Australia (ROM # M37261), and is the same as that studied by Hassan & Grundy (1985). A chemical analysis of the sample gave the following chemical formula: $(Mn_{4.0}Fe_{3.8}Zn_{0.6})[Be_{6.1}Si_{5.8}O_{24}]S_{2.1}$ (Hassan & Grundy 1985). The crystals of danalite were hand-picked and crushed to a powder using an agate mortar and pestle. High-temperature synchrotron X-ray powder-diffraction experiments were performed at beam-line X7B of the National Synchrotron Light Source at Brookhaven National Laboratory. The sample was loaded in a quartz capillary (0.5 mm in diameter, open to air at one end) and was oscillated during the experiment over an angle of 20°. The high-temperature X-ray-diffraction data were collected by using *in situ* synchrotron radiation (λ = 0.92249 Å) at room pressure and from 33 to 1035°C.

Elevated temperatures were obtained using a horseshoe-shaped heater and controlled using a thermocouple element near the capillary. Data were collected at a rate of about 9.5°C/min. The X-ray-diffraction data were collected at regular intervals of about 18°C. The data were collected to a maximum 2θ of about 50° [$(\sin\theta/\lambda) < 0.46$ Å^{-1}]. An imaging plate (IP) detector (Mar345, 2300 × 2300 pixels) mounted perpendicular to the beam path was used to collect full Debye–Scherrer rings with an exposure time of 20 s. Prior to running the sample, a separate experiment using a LaB_6 standard was used to determine the sample-to-detector distance, tilt angle, wavelength, and tilting angle of the IP. The diffraction patterns recorded on the IP were integrated using the Fit2d program (Hammersley 1996).

Rietveld Refinements of the Structure

Of the numerous powder-diffraction patterns collected, twenty-one datasets where chosen at regular intervals for treatment with the Rietveld method, GSAS, and EXPGUI programs (Larson & Von Dreele 2000, Toby 2001). For the room-temperature structure, the starting atomic coordinates, cell parameters, isotropic displacement parameters, and space group, $P\bar{4}3n$, were those of Hassan & Grundy (1985). The refined coordinates of the atoms were then used as input for the next higher-temperature structure. Initially, the idealized chemical formula for danalite was used to constrain the site occupancies in the refinement. The refinement of the site-occupancy factors (*sof*) for the Fe and S atoms indicate this formula to be appropriate. The refined *sof* for the interstitial cations in terms of Fe and S atoms [Fe = 0.983(6) and S = 0.918(9) at 33°C] indicate that the Fe site contains Mn^{2+} cations, and the *sof* for S is underestimated, when compared with the results of the chemical analysis. For the same sample, Hassan & Grundy (1985) found that the *sof* in terms of Fe is 1.06(1), and they set the *sof* for S to be 1.0 in their structure refinement. It should be noted that the *sof* for the Fe site is within 3σ, so this may indicate that the Fe site is fully occupied. In this study, we are interested in changes in the site-occupancy factors of both Fe and S as a function of temperature, so both *sof* were introduced as variables and refined.

In the initial stage, the background was fitted by using the Chebyschev analytical function with 24 coefficients, and the profiles were fitted using the pseudo-Voigt function and an asymmetry correction term (GV, GW, and asym). The zero-shift was set to zero at all temperatures. A full-matrix least-squares refinement varying a scale factor, a cell parameter, atom coordinates, and isotropic displacement parameters converged quickly. Isotropic displacement parameters were used for all the atoms in danalite. Using decreasing weights, soft constraints were used for the *T*–O distances, as we do not expect them to vary with temperature. Because of these constraints, their contribution to χ^2 was about 0.0636 (that is, about 6%) at different temperatures. Finally, the background (24 terms), profile parameters (three terms), a scale factor, and structural parameters (12 variables) were also allowed to vary, and the refinement proceeded to convergence. The number of variables was 40 at the end of the refinement, and the number of observed reflections was 51. The number of observations (data points) was about 2115. The structures refined well at all temperatures. Synchrotron powder X-ray-diffraction patterns are shown in Figure 2, as examples. The cell parameters and the Rietveld structure refinement statistics at various temperatures are listed in Table 1. The coordinates and isotropic displacement parameters of the atoms are given in Table 2, and selected bond-distances and angles are listed in Table 3.

Results and Discussion

Cell parameter

The *a* cell parameter increases linearly with temperature without abrupt changes or discontinuities to 1035°C (Fig. 3). The unit-cell parameter for danalite at 33°C obtained in this study [Table 1; a = 8.23264(5) Å] is slightly different from that obtained at 20°C by Hassan & Grundy (1985: a = 8.2317(9) Å. The a parameter expansion is given by the least-squares fit: $a = 8.2307 +$

TABLE 1. DANALITE: RIETVELD REFINEMENT* AND UNIT-CELL PARAMETER AT VARIOUS TEMPERATURES

T (°C)	a (Å)	R_p	R_{wp}	Exp. R_{wp}	R_F^2	χ^2
SC20§	8.2317(9)					
33	8.23264(5)	0.0146	0.0209	0.0218	0.0322	0.9318
124	8.23606(5)	0.0144	0.0208	0.0218	0.0343	0.9270
142	8.23652(5)	0.0141	0.0205	0.0219	0.0338	0.9000
197	8.23996(5)	0.0141	0.0203	0.0220	0.0344	0.8679
252	8.24186(6)	0.0144	0.0206	0.0220	0.0357	0.8894
306	8.24408(6)	0.0139	0.0199	0.0221	0.0345	0.8270
343	8.24642(6)	0.0139	0.0199	0.0222	0.0361	0.8196
397	8.24837(6)	0.0142	0.0203	0.0223	0.0380	0.8399
452	8.25116(6)	0.0140	0.0201	0.0224	0.0385	0.8202
507	8.25392(6)	0.0132	0.0190	0.0224	0.0350	0.7309
543	8.25445(6)	0.0135	0.0192	0.0225	0.0369	0.7416
598	8.25766(6)	0.0131	0.0188	0.0226	0.0354	0.7076
652	8.26009(6)	0.0134	0.0191	0.0227	0.0373	0.7232
707	8.26256(6)	0.0130	0.0188	0.0228	0.0364	0.6924
744	8.26341(6)	0.0130	0.0188	0.0229	0.0371	0.6876
798	8.26655(6)	0.0128	0.0185	0.0230	0.0372	0.6587
853	8.26863(6)	0.0132	0.0187	0.0230	0.0382	0.6685
907	8.27146(6)	0.0129	0.0185	0.0231	0.0388	0.6499
944	8.27338(6)	0.0131	0.0188	0.0232	0.0382	0.6704
999	8.27569(7)	0.0137	0.0195	0.0233	0.0415	0.7213
1035	8.27725(7)	0.0143	0.0201	0.0234	0.0413	0.7585

* R_p = pattern R factor = $\{\Sigma|(I_o - I_c)|\} / \Sigma I_o$; R_{wp} = weighted pattern R factor = $\{\Sigma[w(I_o - I_c)^2]\} / \Sigma[wI_o^2]\}^{1/2}$, where I_o = observed intensity, I_c = calculated intensity, and $w = 1/I_o$; R_p and R_{wp} are the fitted values obtained without background subtraction; Exp R_{wp} = expected value of $R_{wp} = R_e$. R_F^2 = R-structure factor based on observed and calculated structure-amplitudes = $\{\Sigma|(F_o^{1/2} - F_c^{1/2})|\} / \Sigma F_o^{1/2}$; $\chi^2 = [R_{wp} / R_e]$, where $R_e = [(N - P)/(\Sigma w I_o^2)]^{1/2}$, where N is the number of observations (data points ≈ 1945) and P is the number of variables [a scale factor, background (24), profile (3), and structural parameters (12); total ≈ 40]; $N_{obs.}$ = number of observed reflections = 51.

§ SC20 refers to single-crystal data at 20°C from Hassan & Grundy (1985) in all tables.

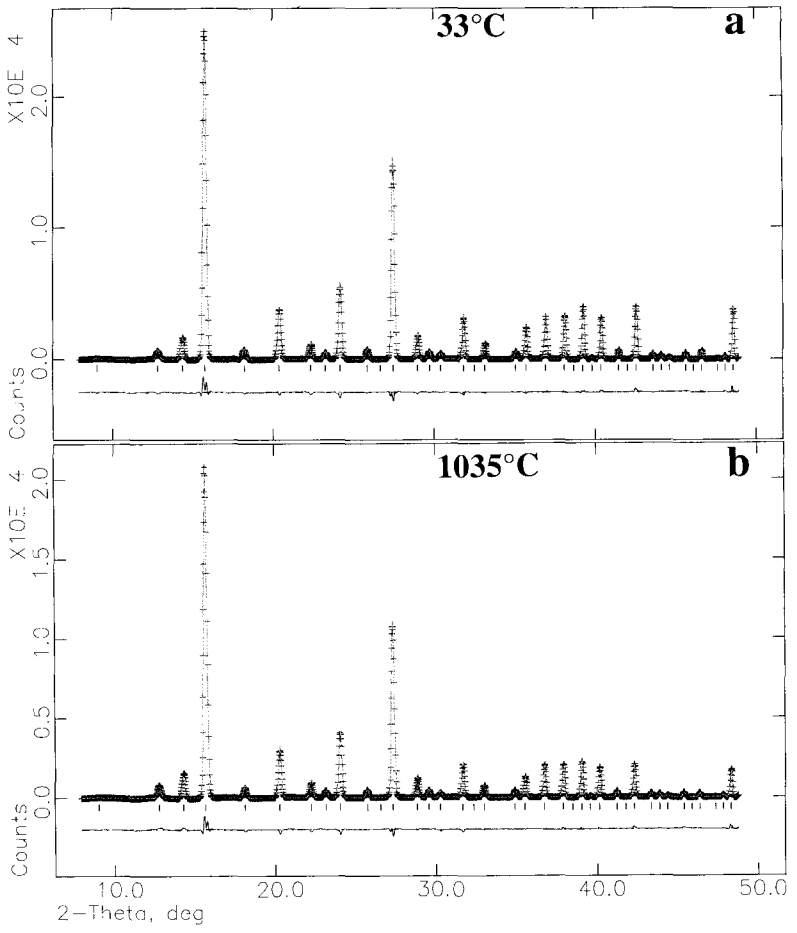

FIG. 2. Synchrotron X-ray powder-diffraction pattern for danalite at 33 and 1035°C, together with the calculated and difference plot from Rietveld refinement. The similarity between the patterns indicates no change in space group.

4.4906×10^{-5}T. The coefficient of linear thermal expansion, $\alpha_a = (da/dT)(1/a)$, calculated from the above equation, varies between 5.455×10^{-6} °C^{-1} at 33°C and 5.425×10^{-6} °C^{-1} at 1035°C. In sodalite, α_a varies between 1.134×10^{-5} °C^{-1} at 28°C and 2.134×10^{-5} °C^{-1} at 982°C (Hassan *et al.* 2004). The volume expansion in danalite is given by the least-squares fit: $V = 557.5692 + 9.1807 \times 10^{-3}$T. The coefficient of volume thermal expansion, $\alpha_V = (dV/dT)(1/V)$ varies between 1.645×10^{-5} °C^{-1} at 33°C and 1.619×10^{-5} °C^{-1} at 1035°C. In sodalite, α_V varies between 3.375×10^{-5} °C^{-1} at 28°C and 6.374×10^{-5} °C^{-1} at 982°C (Hassan *et al.* 2004). The percent volume change between 33 and 1035°C is 1.6(1)% in danalite compared to 4.8(2)% in sodalite between 28 and 982°C. The volume change in danalite is much smaller than in sodalite because of the highly charged $[Fe_4•S]^{6+}$ clusters in danalite compared to $[Na_4•Cl]^{3+}$ in sodalite. Unlike sodalite, the clusters in danalite bond strongly to the framework O atoms, which resist thermal expansion. In addition, the smaller Be atoms in danalite take the place of the larger Al atoms in sodalite. Consequently, danalite is in a more highly collapsed state (*e.g.*, $\varphi_{Si} = 32.11°$ at 33°C) compared to sodalite ($\varphi_{Si} = 23.6°$ at 28°C).

STRUCTURE OF DANALITE

The general structural features of danalite have been described and the structure obtained at 33°C (Fig. 1) is similar to that obtained by Hassan & Grundy (1985). At 33°C, the Be–O and Si–O distances are 1.6359(2) and 1.6293(3) Å, respectively, compared to 1.636(4) and 1.629(4) Å obtained at 20°C by Hassan & Grundy (1985). The Be and Si atoms are fully ordered, so they

TABLE 2. POSITIONAL AND ISOTROPIC DISPLACEMENT PARAMETERS ($U \times 100$ Å^2) AT VARIOUS TEMPERATURES FOR DANALITE

Atom§/T°C		SC20	33	124	142	197	252	306	343	397	452	507
Be	*U*	0.65(21)	1.38(25)	1.57(25)	1.50(25)	1.52(25)	1.64(26)	1.67(25)	1.75(25)	1.70(26)	2.03(27)	1.86(25)
Si	*U*	0.32(5)	1.88(8)	2.09(9)	2.10(8)	2.19(9)	2.26(9)	2.30(9)	2.38(9)	2.44(9)	2.56(9)	2.55(9)
O	*x*	0.1395(4)	0.13936(3)	0.13933(3)	0.13948(3)	0.13947(3)	0.13935(3)	0.13939(3)	0.13947(3)	0.13936(3)	0.13946(3)	0.13971(3)
	y	0.1401(5)	0.13998(3)	0.13995(3)	0.14012(3)	0.14011(3)	0.13998(3)	0.14002(3)	0.14010(3)	0.13999(3)	0.14009(3)	0.14035(3)
	z	0.4126(3)	0.41256(4)	0.41274(4)	0.41282(4)	0.41300(4)	0.41306(4)	0.41320(4)	0.41335(4)	0.41342(4)	0.41361(4)	0.41385(4)
	U	0.66(7)	1.71(8)	2.05(8)	2.05(8)	2.18(8)	2.28(8)	2.36(8)	2.51(8)	2.58(8)	2.68(8)	2.70(8)
Fe	*x*	0.1693(1)	0.16976(6)	0.16992(6)	0.16989(6)	0.16997(6)	0.17003(6)	0.17006(6)	0.17012(6)	0.17017(7)	0.17024(7)	0.17022(6)
	U	0.69(2)	0.60(3)	0.86(3)	0.89(3)	1.08(3)	1.21(3)	1.35(3)	1.41(3)	1.58(3)	1.71(3)	1.89(3)
	sof	1.06(1)	0.983(6)	0.981(6)	0.979(6)	0.980(6)	0.981(6)	0.983(5)	0.979(6)	0.981(6)	0.981(6)	0.985(5)
S	*U*	1.03(7)	1.83(14)	2.05(15)	2.19(15)	2.41(15)	2.60(15)	2.73(15)	2.87(16)	3.10(16)	3.31(16)	3.60(16)
	sof	1.0	0.918(9)	0.920(9)	0.922(9)	0.926(9)	0.928(9)	0.930(9)	0.929(9)	0.933(9)	0.937(9)	0.947(9)

Atom§/T°C		543	598	652	707	744	798	853	907	944	967	1035
Be	*U*	1.84(25)	1.86(25)	2.09(26)	2.21(26)	2.31(26)	2.25(26)	2.31(26)	2.36(26)	2.47(27)	2.59(29)	2.69(30)
Si	*U*	2.56(9)	2.62(9)	2.69(9)	2.69(9)	2.79(9)	2.87(9)	2.83(9)	2.90(9)	2.99(9)	2.85(10)	2.73(10)
O	*x*	0.13965(3)	0.13970(3)	0.13951(3)	0.13954(3)	0.13970(3)	0.13971(3)	0.13960(3)	0.13964(3)	0.13955(3)	0.13894(3)	0.13858(3)
	y	0.14028(3)	0.14034(3)	0.14015(3)	0.14017(2)	0.14033(2)	0.14035(2)	0.14023(2)	0.14028(2)	0.14018(2)	0.13954(3)	0.13916(3)
	z	0.41385(4)	0.41405(4)	0.41412(4)	0.41426(4)	0.41436(4)	0.41454(3)	0.41461(3)	0.41478(3)	0.41485(3)	0.41475(4)	0.41470(4)
	U	2.75(8)	2.87(8)	2.96(8)	3.01(8)	3.09(8)	3.25(8)	3.25(8)	3.36(8)	3.40(9)	3.23(9)	3.08(9)
Fe	*x*	0.17023(6)	0.17022(6)	0.17031(7)	0.17032(7)	0.17033(7)	0.17039(7)	0.17044(7)	0.17044(7)	0.17050(7)	0.17076(7)	0.17093(7)
	U	1.88(3)	2.09(3)	2.15(3)	2.33(3)	2.38(3)	2.53(3)	2.58(3)	2.74(3)	2.82(3)	3.05(4)	3.21(4)
	sof	0.985(5)	0.985(5)	0.985(5)	0.988(5)	0.986(5)	0.984(5)	0.987(5)	0.986(5)	0.986(6)	1.011(6)	1.029(6)
S	*U*	3.51(16)	3.82(16)	3.84(17)	4.06(17)	4.06(17)	4.18(17)	4.22(17)	4.44(17)	4.66(18)	4.22(19)	4.01(19)
	sof	0.942(9)	0.947(9)	0.944(9)	0.951(9)	0.951(9)	0.949(9)	0.950(9)	0.952(9)	0.957(10)	0.943(10)	0.934(10)

§ Si is at (¼, ½, 0), Be is at (¼, 0, ½), Fe is at (x, x, x), and S is at (0, 0, 0).

alternate over the available site in the framework of tetrahedra.

The four identical Be–O bonds have similar lengths to the four identical Si–O bonds (Table 3). The variation of the *T*–O distances shown (Fig. 4a) reveals an abrupt change at 926°C (this temperature is chosen midway between 907 and 944°C), so the data are best described as two groups. For convenience, in all calculations, the value at 944°C was used for the value at 926°C, as there is no value at 926°C. Between 33 and 926°C, the Be–O and Si–O distances are almost constant. Between 926 and 1035°C, the Be–O bond length decreases, whereas the Si–O bond length increases, but the changes are small. In sodalite, between 28 and 982°C, the Si–O and Al–O distances are constant (Hassan *et al.* 2004).

The variation of the angles in the TO_4 tetrahedron is shown in Figure 5. The smaller O–*T*–O angles vary opposite to the larger O*–*T*–O* angles (Figs. 5a, b). Atoms O and O* are framework oxygen atoms related by symmetry. From 33 to 926°C, the Be–O–Si angle increases from 126.11(2) to 127.22(2)° by 1.12(3)°, and from 926 to 1035°C, this angle increases to 127.32(2)°, for a total change of 1.21(3)° (Fig. 5c). In sodalite, from 28 to 982°C, the Al–O–Si bridging angle increases by

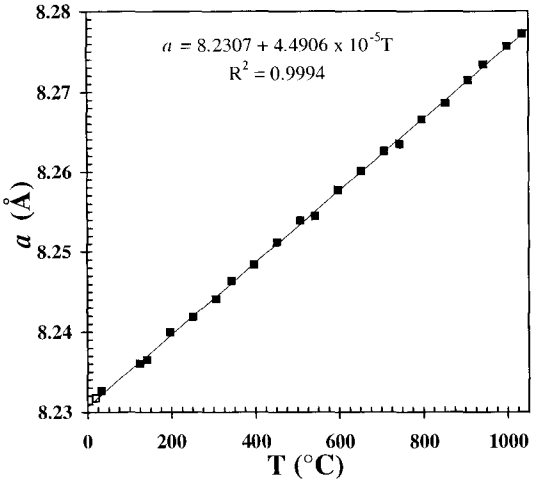

FIG. 3. The *a* unit-cell parameter increases linearly with temperature. The least-squares fit to the data is given as an insert. Error bars are smaller than the symbols. Single-crystal data at 20°C from Hassan & Grundy (1985) are included in all graphs for comparison. They are shown in "opposite" symbols to the present data. Here, the data point is shown as an open square instead of a solid square, and is similarly illustrated in the other graphs.

TABLE 3. BOND DISTANCES (Å) AND ANGLES (°) IN DANALITE AT VARIOUS TEMPERATURES

T (°C)		SC20	33	124	142	197	252	306	343	397	452	507
Be – O	4 ×	1.634(4)	1.6359(2)	1.6358(2)	1.6359(2)	1.6359(2)	1.6359(2)	1.6359(2)	1.6359(2)	1.6359(2)	1.6360(2)	1.6360(2)
O – Be – O	4 ×	108.1(2)	108.06(1)	108.09(1)	108.04(1)	108.06(1)	108.11(1)	108.10(1)	108.08(1)	108.13(1)	108.11(1)	108.04(1)
	2 ×	112.2(2)	112.33(2)	112.27(2)	112.38(2)	112.34(2)	112.24(2)	112.24(2)	112.28(2)	112.18(2)	112.23(2)	112.38(2)
Si – O	4 ×	1.629(4)	1.6293(3)	1.6294(3)	1.6293(3)	1.6293(3)	1.6294(3)	1.6293(3)	1.6293(3)	1.6293(3)	1.6293(3)	1.6293(3)
O – Si – O	4 ×	107.9(2)	108.00(1)	108.03(1)	107.97(1)	107.99(1)	108.04(1)	108.04(1)	108.02(1)	108.07(1)	108.05(1)	107.97(1)
	2 ×	112.6(2)	112.46(2)	112.40(2)	112.51(2)	112.47(1)	112.37(2)	112.37(2)	112.41(2)	112.31(2)	112.36(2)	112.51(1)
Be – O – Si		126.5(2)	126.11(2)	126.20(2)	126.22(2)	126.31(2)	126.36(2)	126.42(2)	126.48(2)	126.54(2)	126.61(2)	126.69(2)
†φ_{Be}		31.96	31.99	31.94	31.89	31.84	31.84	31.80	31.74	31.74	31.66	31.54
φ_{Si}		32.07	32.11	32.06	32.01	31.96	31.96	31.91	31.85	31.85	31.78	31.66
Fe – O	3 ×	2.033(3)	2.0294(5)	2.0308(5)	2.0314(5)	2.0333(5)	2.0340(5)	2.0355(5)	2.0367(5)	2.0377(5)	2.0393(5)	2.0415(5)
Fe – S		2.4132(4)	2.4207(9)	2.4239(9)	2.4236(9)	2.4258(9)	2.4273(9)	2.4283(9)	2.4299(9)	2.4311(9)	2.4330(9)	2.4335(9)

T (°C)		543	598	652	707	744	798	853	907	944	967	1035
Be – O	4 ×	1.6360(2)	1.6360(2)	1.6360(2)	1.6360(2)	1.6360(2)	1.6360(2)	1.6360(2)	1.6360(2)	1.6360(2)	1.6360(2)	1.6360(2)
O – Be – O	4 ×	108.06(1)	108.06(1)	108.13(1)	108.13(1)	108.09(1)	108.10(1)	108.14(1)	108.14(1)	108.18(1)	108.40(1)	108.53(1)
	2 ×	112.33(2)	112.34(2)	112.18(2)	112.18(2)	112.28(2)	112.26(2)	112.17(2)	112.17(2)	112.09(2)	111.63(2)	111.36(2)
Si – O	4 ×	1.6293(3)	1.6293(3)	1.6293(3)	1.6293(3)	1.6293(3)	1.6293(3)	1.6293(3)	1.6293(3)	1.6294(3)	1.6296(3)	1.6297(3)
O – Si – O	4 ×	108.00(1)	108.00(1)	108.07(1)	108.07(1)	108.02(1)	108.03(1)	108.08(1)	108.08(1)	108.12(1)	108.34(1)	108.48(1)
	2 ×	112.46(2)	112.47(1)	112.31(1)	112.31(1)	112.41(1)	112.39(1)	112.30(1)	112.30(1)	112.22(1)	111.75(1)	111.48(2)
Be – O – Si		126.71(2)	126.79(2)	126.86(2)	126.93(2)	126.95(2)	127.04(2)	127.09(2)	127.173(17)	127.22(2)	127.28(2)	127.32(2)
†φ_{Be}		31.55	31.48	31.50	31.45	31.40	31.34	31.34	31.28	31.28	31.42	31.51
φ_{Si}		31.67	31.60	31.62	31.57	31.51	31.45	31.45	31.39	31.39	31.53	31.61
Fe – O	3 ×	2.0418(5)	2.0441(5)	2.0451(5)	2.0467(5)	2.0474(5)	2.0492(5)	2.0503(5)	2.0523(5)	2.0532(5)	2.0526(5)	2.0523(5)
Fe – S		2.4338(9)	2.4347(9)	2.4366(9)	2.4376(9)	2.4379(9)	2.4397(9)	2.4409(10)	2.4419(10)	2.4432(10)	2.4476(10)	2.4506(11)

† No errors are given for the φ angles because they were computed from geometry.

5.06(2)° (Hassan *et al.* 2004). The abrupt change in the structural parameters at 926°C may be explained by oxidation of Fe^{2+} cations and incorporation of O atoms into the structure. Danalite undergoes an oxidation of the Fe^{2+} (and minor Mn^{2+}) cations to the trivalent state beyond 771°C, which is accompanied by a weight gain from the incorporated O atoms, and begins to lose $S_2(g)$ beyond 1029°C, and this is accompanied by a weight loss of $S_2(g)$. Danalite melts at 1274°C, and undergoes another oxidation event of Mn^{3+} to Mn^{4+} cations beyond 1298°C (Antao & Hassan 2002).

Cage Clusters

The β-cages enclose $[Fe_4•S]^{6+}$ clusters that expand with temperature. The orientation of these clusters is fixed by Fe–O bonds to the framework oxygen atoms. The Fe–S bond length increases by 0.023(1) Å from 33 to 926°C, and by 0.007(1) Å from 926 to 1035°C (Fig. 4c). The Fe–O bond distance increases by 0.024(1) Å from 33 to 926°C, and decreases by 0.0009(7) Å from 926 to 1035°C (Fig. 4b). This slight decrease in the Fe–O bond may occur because of oxidation of the Fe^{2+} (and minor Mn^{2+}) cations to the Fe^{3+} (and Mn^{3+}) state and the incorporation of O atoms in the structure (Antao & Hassan 2002). In sodalite, from 28 to 982°C, the $[Na_4•Cl]^{3+}$ clusters expand with increases of the Na–Cl bond length by 0.182(4) Å, and corresponding increases of the short Na–O bond lengths by 0.093(2) Å, and decreases in the longer Na–O* distances by 0.108(1) Å (Hassan *et al.* 2004).

Isotropic Displacement Parameters

The variation of the isotropic displacement parameters, *U*, for the atoms in danalite is displayed in Figure 6a. At 33°C, the *U* values for the atoms are observed in the following order: *U*(Fe) < *U*(Be) < *U*(O) < *U*(S) < *U*(Si). The *U* for the framework atoms increase only slightly with temperature, whereas the *U* for Fe atoms, and S atoms in particular, increase considerably with temperature. The *U* for the S, O, Be and Si atoms decrease beyond 926°C, whereas that for the Fe atoms increases. In sodalite, the *U* values for the interstitial atoms (Na and Cl) increase much more with temperature, compared to the interstitial atoms (Fe and S) in danalite. This is because of the stronger bonds in the $[Fe_4•S]^{6+}$ clusters in danalite compared to the $[Na_4•Cl]^{3+}$ clusters in sodalite; also, the Fe atom is heavier than the Na atom.

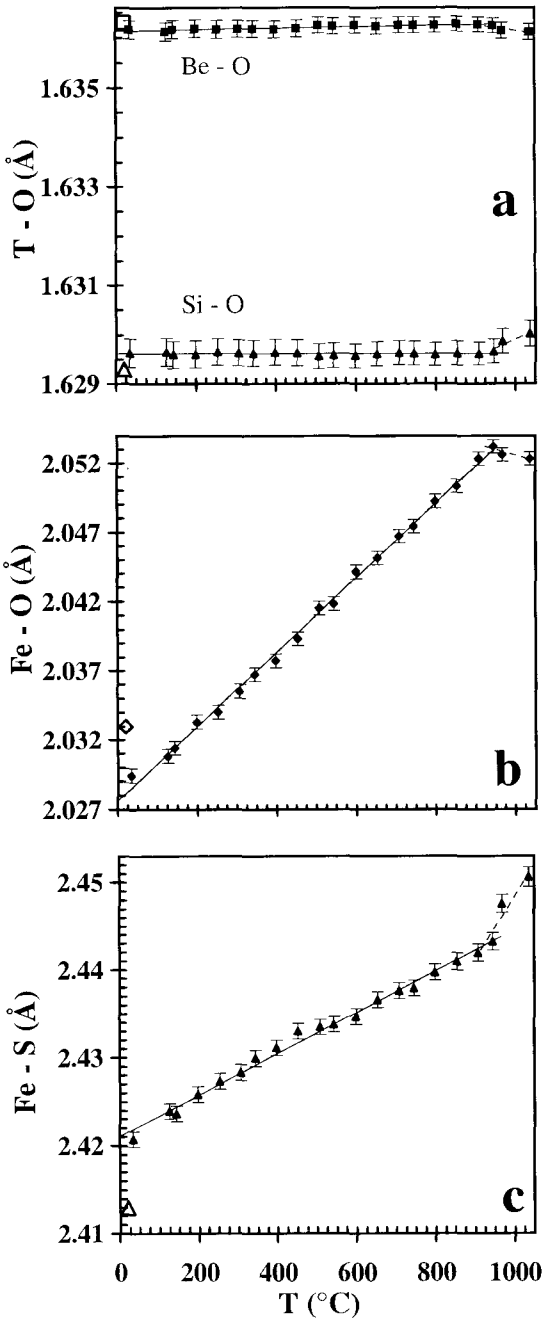

FIG. 4. Variation of the bond distances: (a) *T*–O, (b) Fe–O, and (c) Fe–S with temperature. All distances display an abrupt change at 926°C.

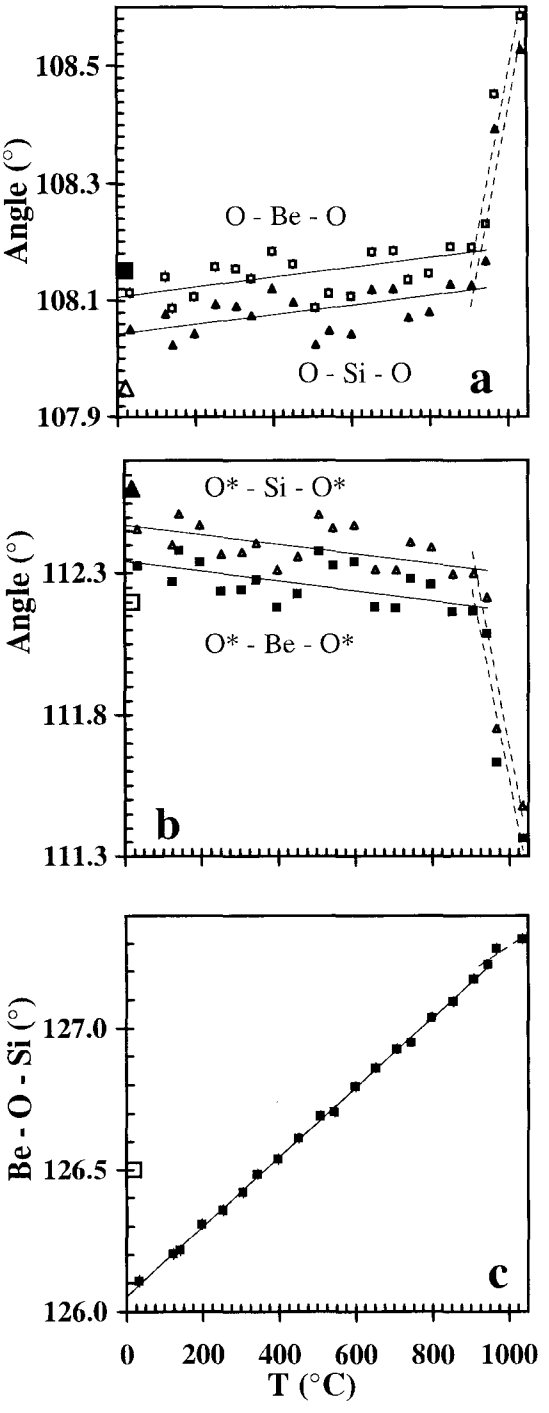

FIG. 5. Variation of the framework TO_4 bond angles (a, b), and (c) Be–O–Si bridging angle with temperature. All angles display an abrupt change at 926°C.

Site-Occupancy Factors for Fe and S Atoms

The values for the site-occupancy factors for Fe are within 3σ of 1.0, indicating that this site may be fully occupied, especially if the errors are underestimated (Table 2). A similar reasoning may be used to indicate that the S site may also be fully occupied. Therefore, the *sof* values for these sites may be set as fully occupied and not refined. In fact, a few structures at different temperatures were refined with fully occupied sites, and the trends we observed for bond lengths and angles were still present. However, we are interested in the *sof* values for the Fe and S sites to check for any systematic trends that may shed some light on the oxidation process that occurs in danalite as it is heated.

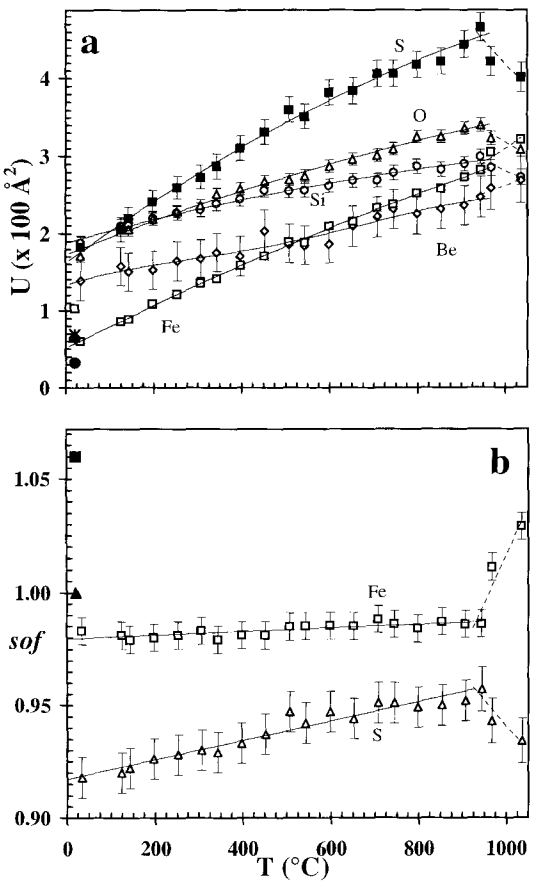

FIG. 6. (a) Variation of the isotropic displacement parameters, U, with temperature. The U values for S increase significantly with temperature. (b) Variation of the *sof* values for the Fe and S atoms with temperature. The *sof* values display an abrupt change at 926°C.

Figure 6b displays the variation of the site-occupancy factor for the Fe atom. The *sof* for Fe remains nearly constant until 926°C, and increases slightly beyond that temperature. The *sof* values are usually correlated with displacement parameters, so these trends may not be realistic. The increase in the *sof* of the S site probably indicates the incorporation of O atoms in the structure as the Fe^{2+} (and minor Mn^{2+}) atoms are oxidized. This increase may also indicate positional disorder of the S and incorporated O atoms. Positional disorder may also occur on the Fe site if it contains Fe^{2+} and Fe^{3+} cations, and may not reflect a true increase in the *sof* for the Fe site. The *sof* for Fe was nearly constant until 926°C, and we do not expect a sudden increase at higher temperatures. The oxidation of Fe^{2+} in danalite is accompanied by a weight gain of 4.0% between 771 and 1029°C (Antao & Hassan 2002). Decrease in the *sof* for the S site above 926°C probably occurs because of the loss of $S_2(g)$. However, the loss of $S_2(g)$ in danalite was observed between 1029 and 1298°C (5.7% weight loss; Antao & Hassan 2002).

The results from this study and that of the thermal analyses agree with each other only in general terms because the temperatures at which significant events occur do differ. This difference in temperature may arise because of different experimental techniques using different rates of heating, sample sizes, and sample environments. In the thermal-analysis study, the loss of $S_2(g)$ in danalite was observed between 1029 and 1298°C, and in the present study, the decrease in the *sof* for the S site occurs between 926 and 1035°C, where the Fe–O bond length shows a small decrease. Oxidation of Fe^{2+} in danalite is accompanied by a weight gain of 4.0% between 771 and 1029°C because of incorporation of O atoms into the structure. In the present study, we observe an increase in the *sof* of S from 33 to 926°C. The concurrent effect of thermal expansion and resulting effect of larger thermal-displacement parameters of the atoms may mask the true *sof* value for the Fe and S atoms. Nevertheless, the results from the two studies are consistent in general terms.

The Mechanism of Thermal Expansion in Danalite

When the geometrical model for the thermal expansion of sodalite (Hassan & Grundy 1984) is combined with the thermal analyses of danalite (Antao & Hassan 2002) and the present results, there results a complete description of the thermal behavior of danalite. In the thermal expansion of danalite, the Fe–S bond expands, which is also indicated by large displacement-parameters for the Fe and S atoms, and this expansion forces the Fe atom toward the plane of the six-membered ring, which causes the framework tetrahedra to rotate. The BeO_4 and SiO_4 tetrahedra rotate by angles φ_{Be} and φ_{Si}, respectively (Fig. 1). These rotational angles are calculated at different temperatures using equation 8 of

Hassan & Grundy (1984), and their variations with temperature are shown (Fig. 7a). Between 33 and 926°C, φ_{Be} and φ_{Si} decrease by about 0.71°. From 926 to 1035°C, φ_{Be} and φ_{Si} increase by about 0.23°. In addition, the framework TO_4 tetrahedra, especially bond angles, change slightly with temperature.

In sodalite, between 28 and 982°C, the angle of rotation of the AlO_4 tetrahedron, φ_{Al}, changes from 22.1 to 16.9° by 5.2°, whereas the angle of rotation of the SiO_4 tetrahedron, φ_{Si}, changes from 23.6 to 18.0° by 5.6°. Therefore, with the larger rotations in sodalite, a higher percentage of expansion is observed in sodalite compared to that in danalite, despite the fact that danalite is in a more collapsed state than sodalite.

As the Fe–S bonds expand, the Fe atoms move along <111> toward the plane of the six-membered rings. The change of the Fe coordinate, x_{Fe}, with the a cell parameter for danalite is given (Fig. 7b). With increasing value of the a parameter, x_{Fe} increases smoothly to 926°C, then it increases sharply to 1035°C. If the Fe atom reaches (¼, ¼, ¼), then it is midway between two S atoms and approximately in the plane of the six-membered ring. The S would then be eight-fold coordinated by eight Fe atoms, and the Fe atom eight-fold coordinated by two S and six framework O atoms, causing the rate of expansion to decrease. In danalite, melting occurs before the Fe atom reaches (¼, ¼, ¼). The maximum value for x_{Fe} [= 0.17093(7)] occurs at the maximum temperature of 1035°C. A comparison of the coordination of the Fe atom and its location with respect to a six-membered ring is shown in Figure 8 for the structures at 33 and 1035°C.

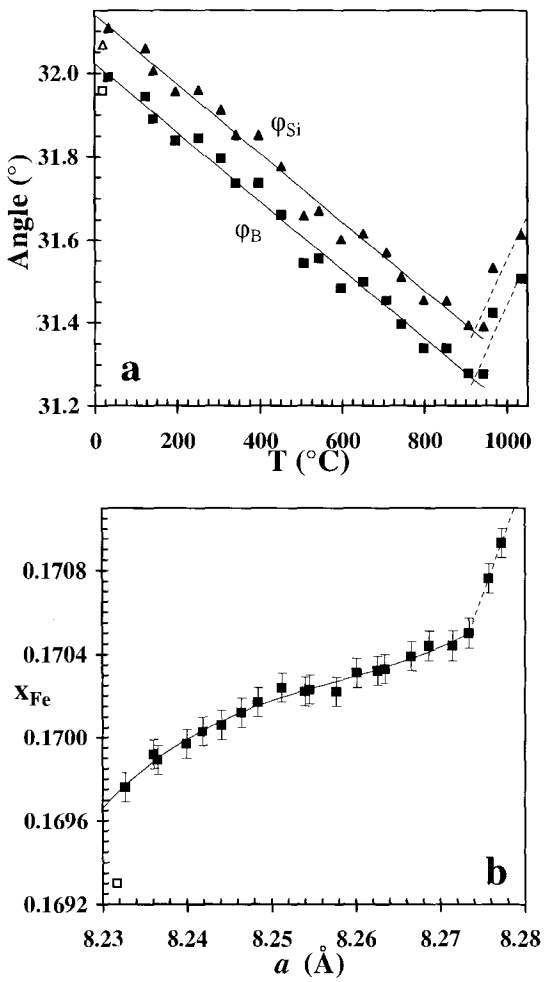

FIG. 7. (a) Variation of the angle of rotation, φ_{Be} and φ_{Si}, of the BeO_4 and SiO_4 tetrahedra, respectively, with temperature (Fig. 1). (b) Variation of the atom coordinate of Fe, x_{Fe}, with a. All values display an abrupt change at 926°C.

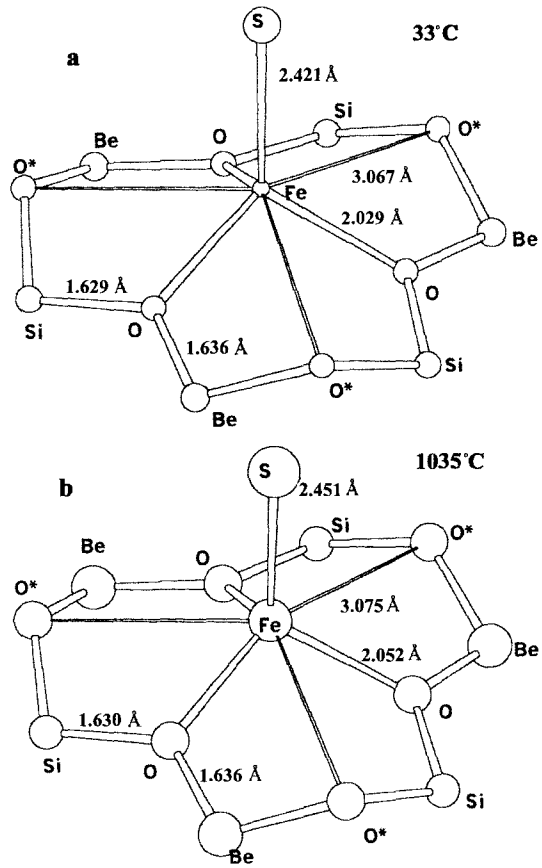

FIG. 8. Comparison of the Fe coordination in danalite at (a) 33°C and (b) 1035°C. The displacement parameters are shown to scale at the 50% probability level. A six-membered ring also is shown. The O* atoms do not form typical Fe–O* bonds, as they are too long.

In this study, synchrotron X-ray powder-diffraction data are combined with thermal data (DTA/TG) to obtain a complete description of the thermal behavior of danalite. The framework in danalite is in a highly collapsed state compared to that in sodalite. In danalite, thermal expansion occurs mainly by expansion of the $[Fe_4•S]^{6+}$ clusters, which causes the framework tetrahedra to rotate slightly. The small change in the angles of rotation of the tetrahedra is reflected by a slight increase in the Be–O–Si bridging angle. In contrast, sodalite contains $[Na_4•Cl]^{3+}$ clusters, and the framework tetrahedra rotate by much larger angles, and the change in the Al–O–Si bridging angle is also larger.

Acknowledgements

Jonathan C. Hanson of Brookhaven National Laboratory is thanked for his help in performing the synchrotron experiments. We thank the Dr. Mauro Prencipe and an anonymous reviewer, as well as Associate Editor Elena Sokolova and Robert F. Martin, for useful comments. Dr. Fred Wicks, Royal Ontario Museum, kindly provided the specimen used in this study. This work was financially supported by a NSF grant to J.B.P., EAR–0125094.

References

Antao, S.M. & Hassan, I. (2002): Thermal analyses of sodalite, tugtupite, danalite, and helvite. *Can. Mineral.* **40**, 163-172.

Barth, T.H.F. (1926): Die kristallographische Beziehung zwischen Helvin und Sodalit. *Norsk Geol. Tidsskr.* **9**, 40-42.

Dunn, P.J. (1976): Genthelvite and the helvine group. *Mineral. Mag.* **40**, 627-636.

Gottfried, C. (1927): Die Raumgruppe des Helvins. *Z. Kristallogr.* **65**, 425-427.

Hammersley, J. (1996): *Fit2d User Manual.* ESRF Publication, Grenoble, France.

Hassan, I., Antao, S.M. & Parise, J.B. (2004): Sodalite: high-temperature structures obtained from synchrotron radiation and Rietveld refinements. *Am. Mineral.* **89**, (in press).

_____ & Grundy, H.D. (1984): The crystal structures of sodalite-group minerals. *Acta Crystallogr.* **B40**, 6-13.

_____ & _____ (1985): The crystal structures of helvite-group minerals, $(Mn,Fe,Zn)_8[Be_6Si_6O_{24}]S_2$. *Am. Mineral.* **70**, 186-192.

_____ & _____ (1991): The crystal structure and thermal expansion of tugtupite, $Na_8[Al_2Be_2Si_8O_{24}]Cl_2$. *Can. Mineral.* **29**, 385-390.

Holloway, W.M., Jr., Giordano, T.J. & Peacor, D.R. (1972): Refinement of the crystal structure of helvite, $Mn_4(BeSiO_4)_3S$. *Acta Crystallogr.* **B28**, 114-117.

Larson, A.C. & Von Dreele, R.B. (2000): *General Structure Analysis System (GSAS).* Los Alamos National Laboratory, Rep. **LAUR 86-748**.

Mel'nikov, O.K., Latvin, B.M. & Fedosova, S.P. (1968): Production of helvite-group compounds *In* Hydrothermal Synthesis of Crystals (A.M. Lobacher, ed.). Nauka, Moscow, Russia (in Russ.).

Pauling, L. (1930): The structure of sodalite and helvite. *Z. Kristallogr.* **74**, 213-225.

Shannon, R.D. (1976): Revised effective ionic radii and systematic studies of interatomic distances in halides and chalcogenides. *Acta Crystallogr.* **A32**, 751-767.

Toby, B.H. (2001): EXPGUI, a graphical user interface for GSAS. *J. Appl. Crystallogr.* **34**, 210-213.

Received April 19, 2003, revised manuscript accepted October 25, 2003.